Published in final edited form as:
Nanotechnology. 2013 December 13; 24(49): 495102. doi:10.1088/0957-4484/24/49/495102.

Surface modification of graphene nanopores for protein translocation

Y. P. Shan[1], **P. B. Tiwari**[1], **P. Krishnakumar**[2], **I. Vlassiouk**[3], **W.Z. Li**[1], **X.W. Wang**[1], **Y. Darici**[1], **S.M. Lindsay**[2,4,5], **H. D. Wang**[6], **S. Smirnov**[7,*], and **J. He**[1,*]

[1]Department of Physics, Florida International University, Miami, FL 33199, USA

[2]Department of Physics, Arizona State University, Tempe, AZ 85287, USA

[3]Oak Ridge National Laboratory, Oak Ridge, TN 37831, USA

[4]Biodesign Institute, Arizona State University, Tempe, AZ 85287, USA

[5]Department of Chemistry and Biochemistry, Arizona State University, Tempe, AZ 85287, USA

[6]State Key Laboratory of Electroanalytical Chemistry, Changchun Institute of Applied Chemistry, Chinese Academy of Sciences, Changchun, Jilin 130022, P.R. China

[7]Department of Chemistry and Biochemistry, New Mexico State University, Las Cruces, NM 88003, USA

Abstract

Studies of DNA translocation through graphene nanopores have revealed their potential for DNA sequencing. Here we report a study of protein translocation through chemically modified graphene nanopores. A transmission electron microscope (TEM) was used to cut nanopores with diameters between 5-20 nm in multilayer graphene prepared by chemical vapor deposition (CVD). After oxygen plasma treatment, the dependence of the measured ionic current on salt concentration and pH was consistent with a small surface charge induced by the formation of carboxyl groups. While translocation of gold nanoparticles (10 nm) was readily detected through such treated pores of a larger diameter, translocation of protein ferritin was not observed either for oxygen plasma treated pores, or for pores modified with mercaptohexadecanoic acid. Ferritin translocation events were reliably observed after the pores were modified with the phospholipid-PEG (DPPE-PEG750) amphiphile. The ion current signature of translocation events was complex, suggesting that a series of interactions between the protein and pore occur during the process.

Keywords

Nanopore; Graphene; surface modification; phospholipid-PEG amphiphile; protein translocation

1. Introduction

Nanopore based analysis is an emerging technique, showing promises in DNA sequencing, genetics, protein analysis and medical diagnostics [1-8]. Advances in nanofabrication allow production of synthetic nanopores in suspended membranes (such as thick silicon nitride thin films and graphene) with controllable pore diameters down to the molecular scale. Thus, individual biomolecules can be analyzed by using a resistive pulse technique in ionic conductance through nanopore, or the Coulter-counting method. The capabilities of these

*Corresponding Author: Sergei, Smirnov, snsm@nmsu.edu; He, Jin, jinhe@fiu.edu..

systems are strongly dependent on the nanopore diameter and the membrane thickness that contains it. Most membranes are much thicker than the size of biomolecules, which limits the sensitivity of synthetic nanopores[9, 10]. In the last three years, graphene attracted a great interest as a novel material for fabricating nanopores [11-13]. Graphene is a single atom thick planar carbon sheet and is mechanically robust so that it can be used as a free standing membrane [14, 15]. Graphene can also stack together with itself or with other sheet materials to form multilayer sandwich structures, which provides a facile way to adjust the geometry and functions of nanopores. Furthermore, graphene is an excellent conductor with high carrier mobility giving it the potential to provide new means to detect the biomolecules electrically and control the electrostatic environment in and near the nanopore. For example, graphene layers can be used as nanoelectrodes [16, 17] for detecting tunneling current or as gate electrodes [18]. These properties make graphene nanopores particular attractive for small biomolecule analysis.

Motivated by the possible application to DNA sequencing, several groups investigated experimentally and theoretically how individual double-stranded DNA (dsDNA) molecules translocate through nanopores in suspended graphene films with diameters in the range 2-25 nm [11-13, 19-26]. These nanopores exhibited remarkable durability in experiments. DNA properties can be revealed based on the statistics of the blocked current during translocation of molecules. These pioneering studies have opened a new area for graphene nanopore - based biomolecule detection and analysis. Recent studies have shown intriguing differences in how DNA translocates through such nanopores with different surface treatments [2], introduced to overcome adsorption of DNA on the graphene surface.

In this report, we used graphene nanopores to study protein translocation, which has not been given much attention to date. Compared to DNA, the interactions between proteins and the graphene surface is stronger and more complicated. For example, recently, Ohno and coworkers [27] reported that bovine serum albumin (BSA) was strongly adsorbed onto graphene with quite a low equilibrium (dissociation) constant $K_D \sim 10^{-8}$ M. Therefore, it is critical to develop new strategies to modify the graphene surface aimed at preventing the non-specific adhesion of proteins. Here, we explored modification of graphene surface by mild oxygen plasma and adsorbing mercaptohexadecanoic acid (C16) and 1,2-dimyristoyl-*sn*-glycero-3-phosphoethanolamine-N-[methoxy(polyethylene glycol)-750] (DPPE-PEG750) molecules. C16 has been successfully used previously for DNA translocation studies [11]. These molecules efficiently adsorb onto the graphene surface and their carboxyl groups, negatively charged at neutral pH, prevent adsorption of DNA molecules [11]. However, we did not observe protein translocation events for such modification and succeeded only when used phospholipids (PL) grafted with polyethylene glycol (PEG), which were previously employed in CNT based biosensors [28]. The two alkyl chains of the PL strongly adhere to hydrophobic surfaces of CNT and graphene while the PEG moieties effectively prevent the non-specific adsorption of proteins. Even in this case, we found that modification of graphene nanopores with DPPE-PEG750 allows reproducible observation of the translocation events for ferritin but not for BSA. The protein translocation was voltage dependent and the translocation time was in the range of tens of milliseconds, much longer than the reported translocation times for kilobase-sized double stranded DNA (dsDNA) [13].

2. Experimental methods

2.1 Chemicals

All chemicals were used without further purification and were purchased from Sigma Aldrich, unless mentioned otherwise, including Ferritin (from Equine spleen, type I). 1,2-dimyristoyl-*sn*-glycero-3-phosphoethanolamine-N-[methoxy(polyethylene glycol)-750] (ammonium salt) (DPPE-PEG750) was purchased from Avanti Polar Lipids (Alabaster, Al);

10 nm gold nanoparticles (NPs, 5.7×10^{12} particles/mL, or 9.5 nM) were purchased from Ted Pella. These gold nanoparticles are capped with negatively charged ligand citrate and the size is very accurate within 10% size variation according to the vendor. All solutions were prepared using deionized (DI) water (~18MΩ) from water purification system (Ultra Purelab system, ELGA/Siemens). Phosphate buffer (PB) was used for measurements at pH 7.0; acetic buffer was used for pH 4.7 and tris buffer was used for pH 9.3. Salt (KCl) at different concentrations was added for experiments on transient ionic conductance caused by translocation of objects through the pore. The salt concentrations were kept low enough to prevent precipitation of the translocation species. For example, gold NPs did not show visible precipitation for [KCl] < 15mM. The ratio between buffer concentration and [KCl] concentration was normally kept at 1:100. The prepared solutions were always filtered through a 0.2 μm filter and degassed by sonication.

2.2 Graphene nanopore fabrication

Fabrication of graphene nanopores was similar to that previously reported procedure [11]. We used multilayer (2-5 layers) graphene due to its higher mechanical stability than the monolayer. Multilayer graphene was grown by chemical vapor deposition (CVD) [29, 30] on Ni (300nm)/SiO_2 (300nm)/Si substrate at ambient pressure in a flow of 2 L/min (in 6 inch split hinge furnace equipped with quartz tube) of methane (0.05%) and hydrogen (1.2%) diluted by argon. The substrate was first annealed in H_2/Ar mixture (2.5%) for 30 min, then the graphene growth was carried at 1000°C for 1 hr and cooled in the same mixture by opening the furnace, which corresponded to the initial rate > 50°C/min. Using the Poly(methyl methacrylate) (PMMA) transfer technique, graphene was suspended over a ~500 nm diameter hole created by a focused ion beam (FIB) in a 300 nm thick silicon nitride (SiN) membrane (Figure 1a-b). The transfer method was slightly modified from the previously reported method [31, 32] and the details are given in the supporting information. The PMMA layer was retained on the graphene during the storage but removed immediately before the transmission electron microscopy (TEM) drilling by immersing the device at least 3 times in dichloromethane and acetone sequentially for 30 seconds each. It was found that residual PMMA is detrimental and a clean graphene surface is critical for preventing amorphous carbon deposition during TEM drilling. An intense and focused electron beam from a TEM (JEOL 2010F, with beam current density 15-20 pA/cm^2 at 200 keV) was used to drill a single nanopore with desirable size in a device with suspended graphene film (Figure 1c).The diameters of most of the resulting pores were between 10-20 nm. After drilling the nanopore, each device was kept in pure ethanol before measurements. Some devices were also cleaned at 400°C in H_2 (390 sccm) and Ar (350 sccm) flow for 1 hour in a tube furnace before measurement but no recognizable effect of that treatment was noticed. We have fabricated more than 50 nanopore devices, out which 20 were functional, *i.e.*, showed ionic conductance within the anticipated range. There are multiple reasons for such a low yield including rupture of the membrane on top of the hole in SiN during transfer or from overexposure in TEM, the above mentioned carbon contaminants that block the pore, and pinholes formation during oxygen plasma treatment (see below). We anticipate that the yield could be dramatically improved.

2.3 Surface modification

Different surface modifications were investigated, all of which were performed on the already prepared nanopore devices. Similar treatments were also analyzed for graphene transferred onto SiO_2/Si substrates. The first one was a gentle treatment by oxygen plasma (7.2 W) for 10-30 seconds. The second one was modification with C16, in which the graphene nanopore device was immersed in 1 mM ethanol solution of C16 at room temperature overnight, then rinsed with DI water for three times and dried in a gentle flow of nitrogen. The third one was modification with DPPE-PEG750, where the devices were

immersed overnight in 1 mg/mL aqueous solution of DPPE-PEG750 at 4 °C, then rinsed with DI water three times, and subsequently dried in a gentle flow of nitrogen. By virtue of the modification conditions, it is expected that sides of the graphene surface in the device are similarly modified.

2.4 Measurements

The experimental setup is sketched in Figure 1d. The fabricated graphene nanopore device was sandwiched between the two identical polydimethylsiloxane (PDMS) microfluidic structures allowing independent liquid flow on both sides of the device (Figure 1e). The sandwich structure is tightly clamped during the experiment. To prevent air bubble formation, ethanol was injected first into the microfluidic system and gradually replaced by water and subsequently by the measurement solution. The measurement setup is placed in a home-built Faraday cage to reduce noise. An Axon 200B (Molecular Devices Inc., CA) in voltage clamp mode is used to supply the bias between the two Ag/AgCl electrodes (MF-2078, BAS, 2M KCl) in two reservoirs, and record the ionic current with a bandwidth of 2-10 kHz. The *cis* side was always grounded and the graphene was electrically floated during the measurements. An Axon Digidata 1440A was used to digitize and record the current signal to a PC at the sampling rate 5 times of the bandwidth. To be consistent, the analytes were typically added in the *cis* side; other than that, the solutions in the *cis* and *trans* sides were identical. We tested the addition of analytes at the *trans* side and no noticeable difference was observed. All the measurements were performed at room temperature. The electrical resistance of the fluidic pathway connecting to the nanopore is at least three orders of magnitude smaller than the resistance of the graphene nanopore and therefore can be ignored. The data were analyzed by Clampfit (Molecular Devices Inc.) and home-built LabView programs.

3. Results and discussion

Graphene is hydrophobic and thus is not easily wetted by water. Attempts to use the graphene nanopore devices without surface modifications were unsuccessful due to poor wetting of the pores. To improve wetting and remove amorphous carbon or other organic contaminations, we first treated the surface of the nanopore device with a low power oxygen plasma. Introduction of oxygen defects renders the graphene surface hydrophilic as can be seen in a drop of the contact angle with water shown in Figure S1. The increase of the number of defects after oxygen plasma treatment was also confirmed by appearance of the D band (~1320 cm^{-1}) in the Raman spectra, which is indicative of disorder and defect in graphene. The spectra before and after the treatment are given in Figure S1.

The ionic conductance, *G*, of each graphene nanopore was measured immediately after the oxygen plasma treatment. As shown in Figure 2a, it depends on the concentration of electrolyte [KCl] nonlinearly, which is indicative of a nonzero surface charge[33, 34]. The nonlinearity is clearly visible up to fairly high salt concentrations, [KCl] < 1 M, which emphasizes that the pore is quite small and the surface charge is relatively high. For pores in a thin membrane, like graphene, the majority of resistance arises from the movement of ions outside the pore, which is described by the so called access resistance; for a pore diameter *d*, in a membrane with neutral walls it corresponds to conductance [13],

$$G = [(\mu_K + \mu_{Cl})\, n_{KCl} e]\, d, \quad (1)$$

where *e* is the electron charge, n_{KCl} is the number concentration of KCl, while μ_K = 7.62 ×10^{-8} m^2/Vs and μ_{Cl} = 7.91 ×10^{-8} m^2/Vs are the mobilities of potassium and chloride ions, respectively. The dashed line in Figure 2a is calculated using eq. (1). Note that it coincides with the experiment at high salt concentration, when the surface charge effects are

diminished. Figure 2b shows that equation 1 fits fairly well the data for 9 graphene nanopores of different diameters measured in 1 M KCl. The deviations are all towards larger effective diameters and are likely due to the increased pore diameters caused by oxygen plasma treatment or some additional pinholes created during this process. Control devices with suspended graphene films but no TEM drilled nanopores occasionally showed small leakage current after the oxygen plasma treatment. A typical result is shown in Figures 3b and c. This current is typically an order of magnitude smaller than the current observed in the devices with 10-20 nm pores and is presumably due to small pinholes generated during the oxygen plasma treatment. This interpretation is supported by the lack of the ionic current spikes in the control devices from translocation of either gold nanoparticles or proteins, as opposed to the intentionally prepared by TEM nanopore devices discussed below.

Concentration dependence of the ionic conductance below 1 M KCl deviated from linear due to a nonzero surface charge that, in a small diameter pore, causes local increase of the counterion concentration. Venkatesan *et al.*[18] used an additional term as the second term in equation 2,

$$G = [(\mu_K + \mu_{Cl})\, n_{KCl} e]\, d + \mu_K \frac{|\sigma_s| \pi d}{L}, \quad (2)$$

to explain concentration dependence of ionic conductance in graphene/alumina sandwiches, where σ_s is the surface charge density and L is the pore length (or thickness of the graphene sandwich). Inclusion of the last term was proposed by Smeets *et al.*[35] for long pores but had a limited success when applied to pores in thin membranes (short pores) [18]. The discrepancy increased with decreasing the aspect ratio for such pores (making the membrane thinner), in line with more generic description given in our previous analysis for pores of different lengths [33, 34]. It can be seen here as well: the best fit using equation 2 with the surface charge density of −39 mC/m^2 (0.25 e/nm^2) and L = 1.5 nm significantly deviates from the experimental data – the conductance does not saturate at low KCl concentrations . Because of the lack of a suitable analytical description, we treated problem numerically following our previously described approach [33, 34]. We showed that the set of Poisson and Nernst-Planck equations (PNP approximation) was sufficient for describing such problems without inclusion of the Navier-Stokes equation and could be applied to analyses of long and short pores with different distribution of charges. Here we also employed PNP approximation and mimicked a pore as a cylindrical cut of a desired diameter in a 1 nm thick membrane, surface of which is uniformly charged on both sides. The best fit, shown in Figure 2a as a red solid line (line 3) illustrates such calculation for 10 nm diameter pore (measured before plasma treatment) with the uniform charge density of −240 mC/m^2 (1.5 e/nm^2). Obviously, this represents a better fit and corresponds to a reasonable surface charge density. This charge density is close to the density of defects that one can estimate based on the intensity ratio of D and G lines, $I_D/I_G \sim 1$ [29, 30]. Some deviations in Figure 2a towards higher currents can be due to a slightly increased pore diameter after the plasma treatment.

Further confirmation of the nature of the surface charge brought about by plasma treatment of graphene comes from the pH dependence of the ionic current through nanopore. High salt concentration (1M KCl) screens the surface charge and diminishes any pH dependence of ionic current. For 1 mM KCl solution, on the other hand, the ionic current is significantly reduced at pH 3.3 as compared to that at higher pH values (Figure S1). It correlates with the anticipated surface charge behavior introduced by carboxyl groups that are neutral around pH 4 and carry negative charge at higher pH. There is no report for pH dependence of ionic current through nanopores in native graphene [11], but the observed pH dependence is very similar to the oxygen plasma treated CNT nanopore [36]. The results are also consistent with the graphene nanopore modified with a positively charged aluminum oxide layer at neutral pH [18].

Before studying protein translocation through graphene nanopores, we first used 10 nm gold nanoparticles (NPs) as a model, since they have a size similar to many proteins. The citrate coated gold NPs have negative charge at pH 7 but we still had to use low salt concentration (10 mM KCl in PB buffer) to prevent their agglomeration. Oxygen plasma treated graphene nanopores with diameters greater than NP size, *i.e.*, 10-20 nm showed the translocation events. A representative one is shown in Figure S3, where current blockades can be seen in the I-t curves, indicating the translocation events of gold NPs through the nanopore. More than 80% of the spikes have a near- rectangular shape, as shown in Figure S3. The spikes only appeared at positive bias. The frequency of spikes is higher at higher applied bias as would be expected for electrophoresis events of the negatively charged NPs. However, these spikes showed very broad distributions both in the width and height that do not strongly depend on bias. We speculate that it is the results of Au NPs aggregation near the graphene nanopore area because the salt concentration was close to macroscopically identifiable NP aggregation. Nevertheless, these results validate the successful realization of graphene nanopore based counter.

Attempts to use such modified nanopores for protein translocation experiments proved unsuccessful, showing that oxygen plasma treatment is insufficient for preventing non-specific protein adsorption onto the graphene surface and thus additional chemical modification is necessary. We have applied two types of self-assembled molecular films, using C16 and DPPE-PEG750 amphiphiles (see their structures in Figure 3a). These molecules can assemble as mono- and probably submono-layers by their hydrophobic tails onto graphene. The carboxyl groups of C16 are negatively charged at neutral pH and have shown to be effective in repelling DNA from assembling on graphene[2]. Thus they would be expected to help in repelling negatively charged proteins but proteins are not uniformly charged as is the case for DNA. Moreover, different peptides significantly vary in their hydrophobicity and charge alone is probably insufficient in preventing protein adsorption. DPPE-PEG750 has a neutral hydrophilic PEG chain, which should be more effective in preventing adsorption of peptides of both charges and different lipophilicities. The successful assembly of C16 and DPPE-PEG750 onto the graphene surface can be confirmed by Electrochemical Impedance Spectroscopy (EIS) applied to similarly treated graphene on solid substrate (Figure S2). After the assembly of DPPE-PEG750, the charge transfer resistance (R_{ct}) from the ($Fe(CN)_6^{-3/-4}$) redox species onto graphene working electrode was increased by almost 130 times, while it increased only 4 times for C16 modification. The increase in R_{ct} indicates successful modification and the greater increase for DPPE-PEG750 indicates that the DPPE-PEG750 molecules can hinder the $Fe(CN)_6^{-3/-4}$ from reaching the graphene surface even better than C16.

The ionic current through a nanopore also decreased slightly after modifying with either C16 or DPPE-PEG750 as is illustrated in Figures 3b and c on a logarithmic scale for measurements in 10 mM KCl at pH 7. The effect is due to a combination of the pore size reduction by the modification and probable covering of pinholes. As shown in Figure 3d, the ionic current retains its pH dependence: it is lower at pH 4.7 and increases with pH for DPPE-PEG750 modified pore in 10 mM KCl. Since there are no ionizable groups in DPPE-PEG750 for this range of pH (pK_a of phosphate is <2) and a similar pH dependence was observed for modifications by C16, we believe that the effect is likely due to the surface groups on graphene generated by the oxygen plasma treatment. Comparing with graphene nanopores only treated with oxygen plasma, we often noticed a larger ionic current variation with time for these C16 and DPPE-PEG750 modified graphene nanopores. For example, the results in Figure 3c and d were obtained from the same graphene nanopore but measured on different days. The ionic current changed from 1nA to 2nA at −0.2V in 10 mM KCl solution (pH 7). This is likely due to the variations of coating molecules over time.

For studying protein transport through chemically modified graphene nanopores, two model proteins were chosen, ferritin and bovine serum albumin (BSA). Ferritin is a glycoprotein produced in equine spleen and has a molecular mass of 440- 450 kDa and isoelectric point (pI) 5.5, *i.e.*, it is negatively charged at neutral pH. Ferritin is very stable and close spherical shape with *ca.* 11 nm diameter. As before with nanoparticles, we had to control the amount of salt (KCl) between 10 mM - 20 mM in PB solution (pH 7.1) to prevent possible agglomeration of ferritin. The concentration of the latter was 0.47 mg/ml. No ferritin translocation signals were observed in C16 modified nanopores; 5 graphene nanopores with diameters in the range of 10-16 nm were measured. Modification with DPPE-PEG 750 was more successful, out of 5 graphene nanopores modified with DPPE-PEG 750, translocation signals were observed in 2 of them. This result suggested that attachment of ferritin to DPPE-PEG 750 modified graphene surface is not significant, which correlates with EIS measurements presented in Figure S2b. Indeed, the R_{ct} for DPPE-PEG 750 modified graphene insignificantly increased (5%) after 1.5 hours incubation with the same concentration of ferritin. In contrast, the R_{ct} of C16 modified graphene increased 40% after at the same conditions. The greater increase of R_{ct} should be attributed to more significant adsorption of ferritin at the surface. Thus we conclude that the C16 modification is not as effective as DPPE-PEG 750 in preventing adsorption of ferritin.

Spikes of current in the I-t dependence were observed only at positive biases when ferritin was added into the *cis* reservoir. At high biases, the ionic current often was too unstable with large low frequency amplitude fluctuations, which may be due to instability of the adsorbed DPPE-PEG750 layer. We thus kept the applied bias below 0.4 V. The downward current spikes are clearly seen at 0.3 V and 0.4 V (as shown in Figure 4a-b) but no identifiable events were detected at 0.2 V or lower. More spikes appeared at 0.4V (the capture rate = 0.22 events/s) than at 0.3V (the capture rate = 0.15 events/s). Three representative spikes at 0.4 V are shown in Figure 4c. Notably, the shape of the spikes showed significant variations, which is very different from more reproducible rectangular spikes for 10 nm gold nanoparticle (Figure S3c). To confirm that these spikes are due to the translocation of negatively charged ferritin, we switched the bias to −0.3 V and −0.4 V and no spikes were observed, as shown in the inset of Figure 4a. The event distribution plot for ferritin translocation at the two biases is shown in Figure 4d. The amplitude of the current spikes increases with the bias increasing from 0.3 V to 0.4 V. It is accompanied by reduction of the translocation time from 60 ± 20 ms to 20 ± 10 ms. The observed voltage dependence of blockage current amplitude is consistent with the characteristics of blockage current [37, 38]. However, the negative surface charge at the graphene surface should also play a role here because no spikes were observed below 0.2V. The strong voltage dependence of translocation time implies that the protein translocation is mainly due to electrophoresis but with a much stronger dependence on the bias. A small subset of proteins at 0.4V shows a slower translocation (90 ± 20 ms) which may be attributed to a population of proteins that interact more strongly with the graphene edges.

The measured protein translocation times are significantly longer than the translocation times of kilobase-ranged dsDNA[13] and even of λ-DNA[11, 12] that is 48.5 thousand base pairs (or 32.7 MDa). It should not be surprising since the mobility of proteins is significantly smaller -- they have a larger radius and a much smaller charge. Besides, the interaction between protein and the graphene edges or surface can be much stronger as some amino acids are quite lipophilic. The stronger interaction should also induce more complex spike shapes.

We were unable to observe reproducible translocation events for another protein, BSA. BSA is a 607 amino acids (69 kDa) serum protein with pI of 4.8, *i.e.*, it is also negatively charged at neutral pH. It is smaller than ferritin and has a prolate shape (14 nm in length and 4 nm in

diameter, see Figure 1d). No reproducible translocation signals were observed for this protein at any bias in the range from −0.7 V to +0.7 V for any of the listed modifications. It is likely due to the prolate shape and low charge of the protein, for which the signal is too small and too short for unambiguous identification in large (>10 nm diameter) pores[39] while stronger interaction between BSA and the graphene surface for smaller pore diameters prevents its translocation.

4. Conclusions

In summary, we have successfully fabricated single nanopores in multilayer graphene and investigated the effect of different modification methods on ionic conductance and protein translocation. It has been found that mild oxygen plasma treatment can be used to improve wetting. It causes the graphene surface to gain negative charge that is seen as lowering of the contact angle and weaker conductance dependence on salt concentration. Translocation of gold nanoparticles through such treated nanopores was observed as spikes in ionic conductance. Nevertheless, this modification was insufficient in preventing protein adsorption onto the graphene surface and for the protein translocation events, additional treatment was required. Modification with DPPE-PEG750 better serves this role due to the lipophilic but neutral PEG group. The translocation of (spherically shaped) protein ferritin was observed only for DPPE-PEG750 modified graphene nanopores and showed strong voltage dependence of the translocation time, which is much longer than for DNA of similar or larger size. The effect is sensitive to the protein size and shape as no translocation events were detected for another protein, BSA. More robust chemical modification methods are needed for successful application of this technique to other proteins. It may also include attachment of receptor molecules at the edge of the graphene nanopores to enhance the discrimination of proteins in the ionic readout signal [40, 41].

Supplementary Material

Refer to Web version on PubMed Central for supplementary material.

Acknowledgments

We acknowledge the use of nanofab at the Center for Solid State Electronic Research (CSSER) and SEM and TEM at the Center for Solid State Science (CSSS) at Arizona State University, and the nanofab at AMERI at Florida International University (FIU). This work was supported by the start-up funds and 2012 faculty summer research award (J.H) from FIU CAS and the DNA Sequencing Technology Program of the National Human Genome Research Institute (1RC2HG005625-01, 1R21HG004770-01). P. Tiwari would also like to thank FIU School of Integrated Science & Humanity, College Arts & Sciences for the research assistantship. A portion of this research was conducted at the Center for Nanophase Materials Sciences, which is sponsored at Oak Ridge National Laboratory by the Scientific User Facilities Division, Office of Basic Energy Sciences, U.S. Department of Energy.

References

1. Branton D, Deamer DW, Marziali A, Bayley H, Benner SA, Butler T, Di Ventra M, Garaj S, Hibbs A, Huang XH, Jovanovich SB, Krstic PS, Lindsay S, Ling XSS, Mastrangelo CH, Meller A, Oliver JS, Pershin YV, Ramsey JM, Riehn R, Soni GV, Tabard-Cossa V, Wanunu M, Wiggin M, Schloss JA. The potential and challenges of nanopore sequencing. Nat. Biotechnol. 2008; 26:1146–53. [PubMed: 18846088]
2. Venkatesan BM, Bashir R. Nanopore sensors for nucleic acid analysis. Nat Nano. 2011; 6:615–24.
3. Firnkes M, Pedone D, Knezevic J, Döblinger M, Rant U. Electrically Facilitated Translocations of Proteins through Silicon Nitride Nanopores: Conjoint and Competitive Action of Diffusion, Electrophoresis, and Electroosmosis. Nano Letters. 2010; 10:2162–7. [PubMed: 20438117]
4. Gu L-Q, Shim JW. Single molecule sensing by nanopores and nanopore devices. Analyst. 2010; 135:441–51. [PubMed: 20174694]

5. Movileanu L. Interrogating single proteins through nanopores: challenges and opportunities. Trends in Biotechnology. 2009; 27:333–41. [PubMed: 19394097]
6. Howorka S, Siwy Z. Nanopore analytics: sensing of single molecules. Chemical Society Reviews. 2009; 38:2360–84. [PubMed: 19623355]
7. Han A, Creus M, Schurmann G, Linder V, Ward TR, de Rooij NF, Staufer U. Label-Free Detection of Single Protein Molecules and Protein-protein Interactions Using Synthetic. Nanopores Analytical Chemistry. 2008; 80:4651–8.
8. Daniel F, Bradley L, David SM, Jiali L. Electrical characterization of protein molecules by a solid-state nanopore. Applied Physics Letters. 2007; 91:053901.
9. Wanunu M, Dadosh T, Ray V, Jin J, McReynolds L, Drndic M. Rapid electronic detection of probe-specific microRNAs using thin nanopore sensors. Nat Nano. 2010; 5:807–14.
10. Siwy ZS, Davenport M. Nanopores: Graphene opens up to DNA. Nat Nano. 2010; 5:697–8.
11. Schneider G g F, Kowalczyk S W, Calado V E, Pandraud G g, Zandbergen HW, Vandersypen LMK, Dekker C. DNA Translocation through Graphene Nanopores. Nano Letters. 2010; 10:3163–7. [PubMed: 20608744]
12. Merchant CA, Healy K, Wanunu M, Ray V, Peterman N, Bartel J, Fischbein MD, Venta K, Luo Z, Johnson ATC, Drndić M. DNA Translocation through Graphene Nanopores. Nano Letters. 2010; 10:2915–21. [PubMed: 20698604]
13. Garaj S, Hubbard W, Reina A, Kong J, Branton D, Golovchenko JA. Graphene as a subnanometre trans-electrode membrane. Nature. 2010; 467:190–3. [PubMed: 20720538]
14. Meyer JC, Geim AK, Katsnelson MI, Novoselov KS, Booth TJ, Roth S. The structure of suspended graphene sheets. Nature. 2007; 446:60–3. [PubMed: 17330039]
15. Tsoukleri G, Parthenios J, Papagelis K, Jalil R, Ferrari AC, Geim AK, Novoselov KS, Galiotis C. Subjecting a Graphene Monolayer to Tension and Compression. small. 2009; 5:2397–402. [PubMed: 19642092]
16. Postma HWC. Rapid Sequencing of Individual DNA Molecules in Graphene Nanogaps. Nano Letters. 2010; 10:420–5. [PubMed: 20044842]
17. Prasongkit J, Grigoriev A, Pathak B, Ahuja R, Scheicher RH. Transverse Conductance of DNA Nucleotides in a Graphene Nanogap from First Principles. Nano Letters. 2011; 11:1941–5. [PubMed: 21495701]
18. Venkatesan BM, Estrada D, Banerjee S, Jin X, Dorgan VE, Bae M-H, Aluru NR, Pop E, Bashir R. Stacked Graphene-Al2O3 Nanopore Sensors for Sensitive Detection of DNA and DNA– Protein Complexes. ACS Nano. 2011; 6:441–50. [PubMed: 22165962]
19. Avdoshenko SM, Nozaki D, Gomes da Rocha C, González JW, Lee MH, Gutierrez R, Cuniberti G. Dynamic and Electronic Transport Properties of DNA Translocation through Graphene Nanopores. Nano Letters. 2013; 13:1969–76. [PubMed: 23586585]
20. Sathe C, Zou X, Leburton J-P, Schulten K. Computational Investigation of DNA Detection Using Graphene Nanopores. ACS Nano. 2011; 5:8842–51. [PubMed: 21981556]
21. Wells DB, Belkin M, Comer J, Aksimentiev A. Assessing Graphene Nanopores for Sequencing DNA. Nano Letters. 2012; 12:4117–23. [PubMed: 22780094]
22. Nelson T, Zhang B, Prezhdo OV. Detection of Nucleic Acids with Graphene Nanopores: Ab Initio Characterization of a Novel Sequencing Device. Nano Letters. 2010; 10:3237–42. [PubMed: 20722409]
23. Saha KK, Drndić M, Nikolić BK. DNA Base-Specific Modulation of Microampere Transverse Edge Currents through a Metallic Graphene Nanoribbon with a Nanopore. Nano Letters. 2011; 12:50–5. [PubMed: 22141739]
24. Massimiliano Di V. Fast DNA sequencing by electrical means inches closer. Nanotechnology. 2013; 24:342501. [PubMed: 23899780]
25. Guohui H, Mao M, Sandip G. Ion transport through a graphene nanopore. Nanotechnology. 2012; 23:395501. [PubMed: 22962262]
26. Mao M, Sandip G, Guohui H. Hydrodynamic flow in the vicinity of a nanopore induced by an applied voltage. Nanotechnology. 2013; 24:245202. [PubMed: 23689946]

27. Ohno Y, Maehashi K, Yamashiro Y, Matsumoto K. Electrolyte-Gated Graphene Field-Effect Transistors for Detecting pH and Protein Adsorption. Nano Letters. 2009; 9:3318–22. [PubMed: 19637913]
28. Liu Z, Winters M, Holodniy M, Dai H. siRNA Delivery into Human T Cells and Primary Cells with Carbon-Nanotube Transporters. Angewandte Chemie International Edition. 2007; 46:2023–7.
29. Vlassiouk I, Smirnov S, Ivanov I, Fulvio PF, Dai S, Meyer H, Chi M, Hensley D, Datskos P, Lavrik NV. Electrical and thermal conductivity of low temperature CVD graphene: the effect of disorder. Nanotechnology. 2011; 22:275716. [PubMed: 21613685]
30. Vlassiouk I, Regmi M, Fulvio P, Dai S, Datskos P, Eres G, Smirnov S. Role of Hydrogen in Chemical Vapor Deposition Growth of Large Single-Crystal Graphene. ACS Nano. 2011; 5:6069–76. [PubMed: 21707037]
31. Li X, Zhu Y, Cai W, Borysiak M, Han B, Chen D, Piner RD, Colombo L, Ruoff RS. Transfer of Large-Area Graphene Films for High-Performance Transparent Conductive Electrodes. Nano Letters. 2009; 9:4359–63. [PubMed: 19845330]
32. Schneider GF, Calado VE, Zandbergen H, Vandersypen LMK, Dekker C. Wedging Transfer of Nanostructures. Nano Letters. 2010; 10:1912–6. [PubMed: 20402493]
33. Vlassiouk I, Smirnov S, Siwy Z. Ionic Selectivity of Single Nanochannels. Nano Letters. 2008; 8:1978–85. [PubMed: 18558784]
34. Vlassiouk I, Smirnov S, Siwy Z. Nanofluidic Ionic Diodes. Comparison of Analytical and Numerical Solutions. ACS Nano. 2008; 2:1589–602. [PubMed: 19206361]
35. Smeets RMM, Keyser UF, Krapf D, Wu M-Y, Dekker NH, Dekker C. Salt Dependence of Ion Transport and DNA Translocation through Solid-State Nanopores. Nano Letters. 2005; 6:89–95. [PubMed: 16402793]
36. Liu H, He J, Tang J, Liu H, Pang P, Cao D, Krstic P, Joseph S, Lindsay S, Nuckolls C. Translocation of Single-Stranded DNA Through Single-Walled Carbon. Nanotubes Science. 2010; 327:64–7.
37. Chen P, Gu J, Brandin E, Kim Y-R, Wang Q, Branton D. Probing Single DNA Molecule Transport Using Fabricated Nanopores. Nano Letters. 2004; 4:2293–8.
38. Talaga DS, Li J. Single-Molecule Protein Unfolding in Solid State Nanopores. Journal of the American Chemical Society. 2009; 131:9287–97. [PubMed: 19530678]
39. Plesa C, Kowalczyk SW, Zinsmeester R, Grosberg AY, Rabin Y, Dekker C. Fast Translocation of Proteins through Solid State Nanopores. Nano Letters. 2013; 13:658–63. [PubMed: 23343345]
40. Garaj S, Liu S, Golovchenko JA, Branton D. Molecule-hugging graphene nanopores. Proceedings of the National Academy of Sciences. 2013
41. He Y, Scheicher RH, Grigoriev A, Ahuja R, Long S, Huo Z, Liu M. Enhanced DNA Sequencing Performance Through Edge-Hydrogenation of Graphene Electrodes. Advanced Functional Materials. 2011; 21:2674–9.

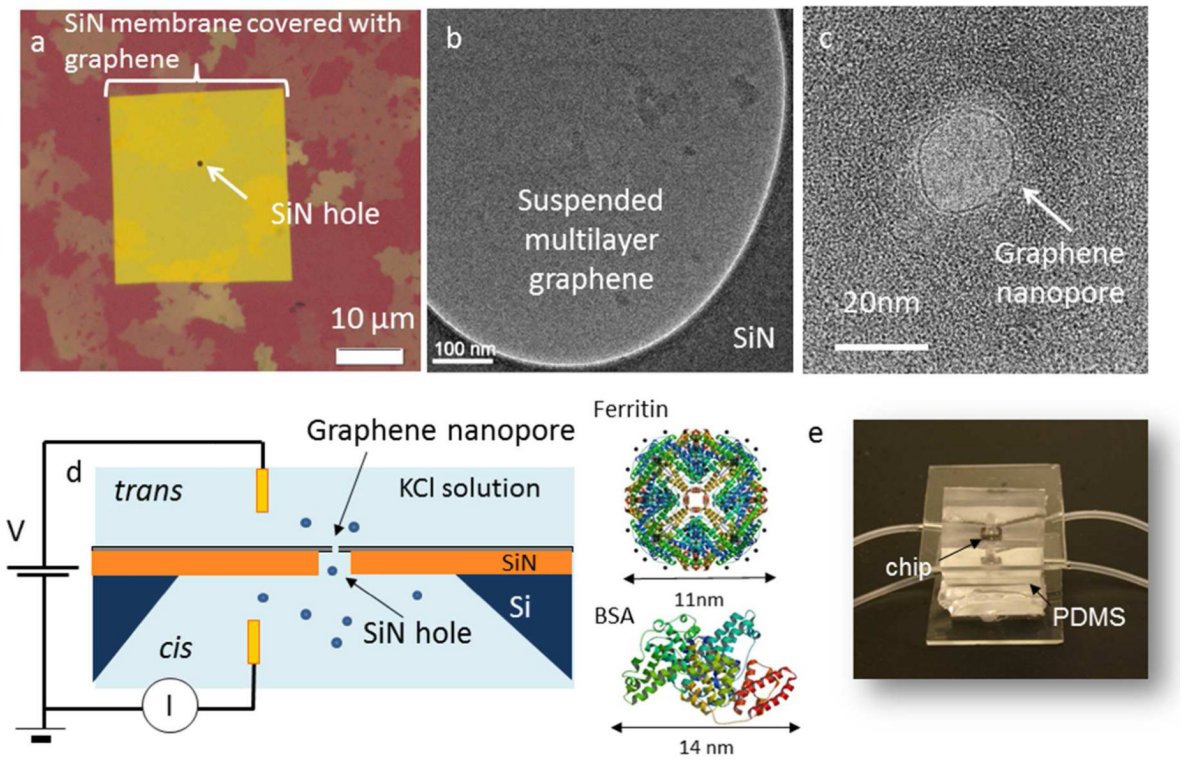

Figure 1.

Illustration of the graphene nanopore devices: (a) optical microscope image of graphene on top of the SiN membrane (yellow rectangle) that has a hole (black dot) drilled by FIB; (b) low resolution Transmission electron microscopy (TEM) image of graphene suspended on top of the hole in SiN membrane; (c) high resolution TEM image of a typical nanopore drilled in suspended graphene by TEM; (d) sketch of the experimental setup and the biological assembly images of Ferritin and BSA (from RCSB Protein Data Bank); (e) a digital photograph of the assembly with two PDMS microfluidic pieces.

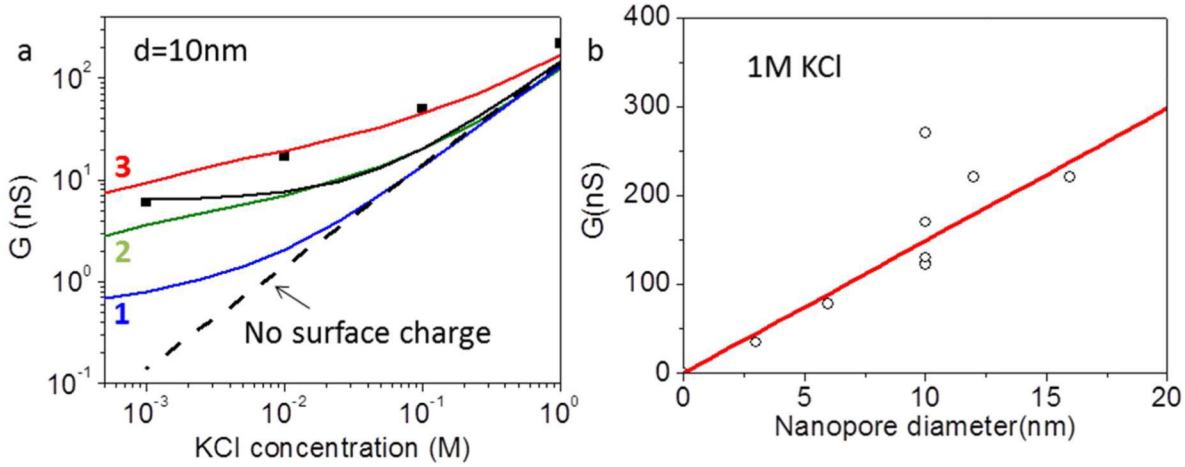

Figure 2.

(a) Salt concentration dependence of the conductance through an oxygen plasma treated graphene nanopore (10 nm diameter) at pH=7 (solid black squares). The dashed line illustrates the theoretical dependence (eq.(1)) for such diameter at zero surface charge. The departure from it is due to a modest surface charge that graphene gains as a result of oxygen plasma treatment. The black solid line is the best fitting by eq.(2) with a surface charge density $\sigma_s = -39$ mC/m^2. The blue (1), green (2) and red (3) solid lines are calculated by a set of Poisson and Nernst-Planck equations with $\sigma_s = -16$, -80 and -240 mC/m^2 respectively. (b) Dependence of the conductance through oxygen plasma treated graphene nanopores on their diameter in 1 M KCl and pH=7. The solid line corresponds to the theoretical prediction from eq.(1).

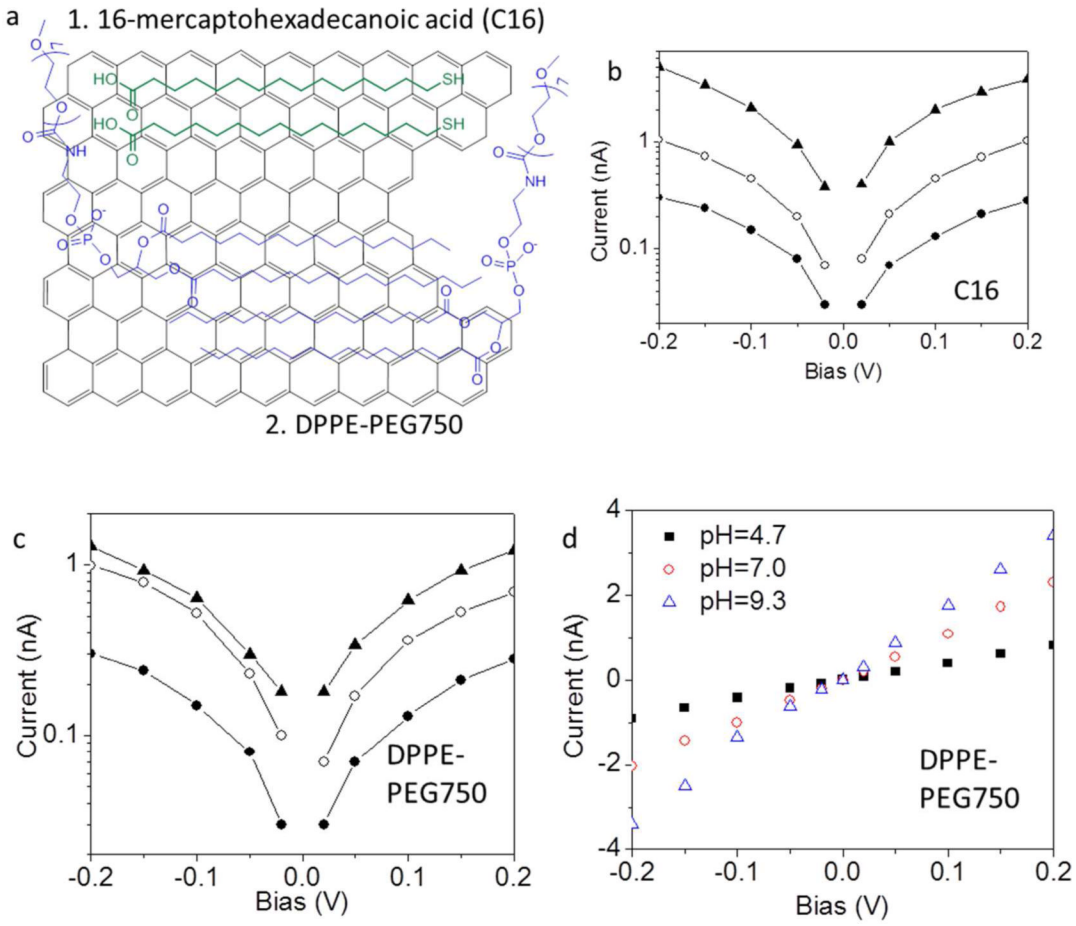

Figure 3.

The electrical measurements of chemically modified graphene nanopores. (a) Illustration of the possible modes of assembling C16 (1) and DPPE-PEG750 (2) on graphene. The semi-log ionic current-voltage (I-V) characteristics of C16 (b) and DPPE-PEG750 (c) modified graphene nanopore devices before (solid triangle) and after (open circle) the chemical modifications. The diameters of the pores are 16 nm and 9 nm respectively. The semi-log I-V curve of a graphene membrane without nanopore (different sample) after 10 seconds of oxygen plasma treatment is shown as a reference (solid circle). Absolute values of the current are used in the semi-log IV curves. (d) The I-V curves of a DPPE-PEG750 modified graphene nanopore (same device as in (c)) at different pH. The ionic current measurements were performed in 10 mM KCl solution in both cases.

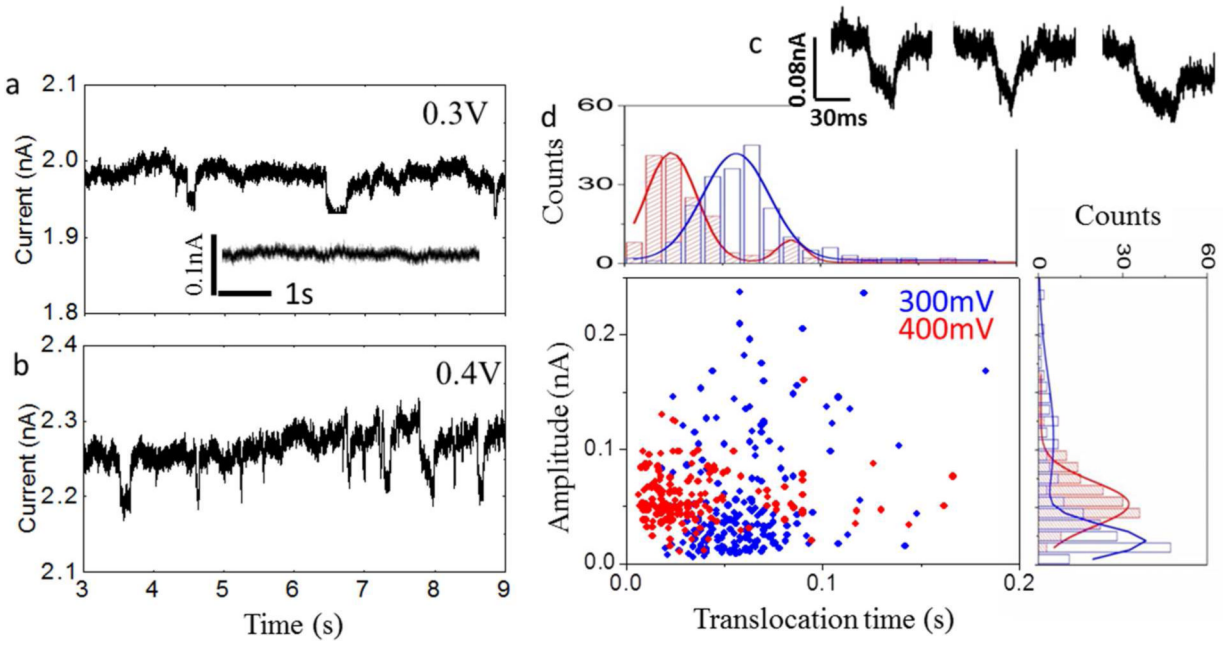

Figure 4.

The ferritin translocation experiments at different biases. Current-time (I-t) traces at 0.3V(a) and 0.4V (b) after the addition of 0.47mg/mL ferritin protein into the *cis* reservoir. The inset in (a) shows a current trace before adding the ferritin. (b) An I-t trace shows the ferritin translocation events (downward current spikes) at 0.4V. (c) Three representative current spikes at 0.4V on a shorter time scale. (d) A scatter plot of the current spike amplitudes versus spike width (translocation time) at different applied bias (blue, 300mV, red, 400mV). The histograms of the spike heights and widths are shown at the scatter plot top and right sides respectively. The spikes with amplitude two times higher than the baseline noise were selected as translocation events. The solid lines in the histograms are Gaussian fits. The diameter of the graphene nanopore is about 16nm. All the measurements were performed in 10mM PB (pH=7.1).